POLITECNICO DI TORINO
Repository ISTITUZIONALE

Frequency-Domain Characterization of Power Inductors for Class-E Resonant Converters

Original
Frequency-Domain Characterization of Power Inductors for Class-E Resonant Converters / Bacmaga, J.; Blecic, R.; Pareschi, F.; Rovatti, R.; Setti, G.; Baric, A.. - STAMPA. - 2019:(2019), pp. 1-4. (Intervento presentato al convegno 23rd IEEE Workshop on Signal and Power Integrity, SPI 2019 tenutosi a Chambery (France) nel June 18-21, 2019) [10.1109/SaPIW.2019.8781682].

Availability:
This version is available at: 11583/2786313 since: 2021-08-19T18:18:46Z

Publisher:
Institute of Electrical and Electronics Engineers Inc.

Published
DOI:10.1109/SaPIW.2019.8781682

Terms of use:

This article is made available under terms and conditions as specified in the corresponding bibliographic description in the repository

Publisher copyright
IEEE postprint/Author's Accepted Manuscript

©2019 IEEE. Personal use of this material is permitted. Permission from IEEE must be obtained for all other uses, in any current or future media, including reprinting/republishing this material for advertising or promotional purposes, creating new collecting works, for resale or lists, or reuse of any copyrighted component of this work in other works.

(Article begins on next page)

12 October 2024

This is the author's version of the article that has been presented at IEEE SPI2019
The editorial version of the paper is available at http://dx.doi.org/10.1109/SaPIW.2019.8781682

Frequency-Domain Characterization of Power Inductors for Class-E Resonant Converters

Josip Bačmaga*, Raul Blečić*, Fabio Pareschi†‡, Riccardo Rovatti‡§, Gianluca Setti†‡, Adrijan Barić*
*University of Zagreb, Faculty of Electrical Engineering and Computing, Unska 3, 10000 Zagreb, Croatia
Tel: +385 (0)1 6129547, e-mail: josip.bacmaga@fer.hr
†Department of Electronics and Telecommunications, Politecnico di Torino, 10129 Torino, Italy
‡Advanced Research Center on Electronic Systems (ARCES), University of Bologna, 40125 Bologna, Italy
§Department of Electrical, Electronic and Information Engineering (DEI), University of Bologna, 40136 Bologna, Italy

***Abstract*—Inductance and Q factor of the ferrite-core shielded power inductors are extracted from two-port S-parameter measurements in the frequency range from 500 kHz to 100 MHz. Seventeen power inductors are chosen to investigate the impact of the different manufacturer, inductance and saturation current rating on the extracted characteristics. The impact of the inductance and Q factor on the operation of the class-E resonant converter is analyzed by the time-domain simulations. The output voltage of the converter largely depends on the Q factor and inductance of the power inductor used in the design methodology.**

***Index Terms*—Q factor, S-parameters, self resonant frequency, switching power supplies, two-port measurements.**

I. Introduction

The main advantage of resonant switching converters over the non-resonant ones is the ability to satisfy the zero-voltage-switching (ZVS) and zero-voltage-derivative-switching (ZVDS) events which significantly reduces the switching losses [1], [2]. The operation of the resonant converters is typically largely dependent on the parasitics of the inductors and capacitors that are used in the design, such as the quality (Q) factor of the power inductors. As an example, the Q factor of the power inductors is one of the input parameters for the state-of-the-art design methodology for the class-E resonant converters [1] and the accurate estimation of the Q factor is necessary to predict the operation of such converters.

The Q factor can significantly vary depending on many inductor parameters, such as inductor case size or the core material, i.e. manufacturer of the inductor. The Q factor of the power inductor against the frequency for the on-chip spiral inductors is analyzed in [3]. However, there is a lack of papers that present an impact of power inductor characteristics on the operation of resonant switching converters.

This paper presents the extracted Q factor values for seventeen power inductors typically used in switching converters. The inductors are chosen from different manufacturers and with various inductances and saturation current ratings (case sizes). The Q factor is extracted from the S-parameter measurements using the "shunt" measurement method that has been proposed as an accurate characterization method for low-impedance components [4], [5]. The impact of the inductor parameters on the operation of the class-E resonant converter is investigated by the time-domain simulations.

Section II presents the characterization method. The measured inductor parameters are shown in Section III, while their impact on the operation of the class-E resonant converter is discussed in Section IV. Section V concludes the paper.

II. Characterization Method

The two-port measurement setup is designed for the S-parameter characterization of the analyzed power inductors, while two calibration structures are processed to extract the parasitics of the test fixture. All the structures are designed on dual-sided PCB using the 50-Ω conductor-backed coplanar waveguide (CBCPW) transmission lines [6]. The parameters of the CBCPW lines are center strip width (1.26 mm), center strip thickness (0.035 mm), gap between the center strip and surrounding ground planes (0.254 mm) and dielectric thickness (1.5 mm). All measurements are performed in the frequency range from 500 kHz to 100 MHz by the vector network analyzer (VNA) R&S ZVB8. The bias current of the characterized inductors is 0 A.

A. Devices under test

The devices under test (DUTs) are the ferrite-core shielded power inductors chosen by different inductor characteristics and divided into three sets. The parameter that is varied in each of the three chosen sets is:

1) manufacturer ($L = 1$ μH, $I_{sat} > 8$ A): #1 – #4,
2) inductance (same inductor series): #5 – #14,
3) saturation current, i.e. case size ($L = 1$ μH): #15 – #18.

All the inductors are chosen to have a root-mean-square (RMS) current rating larger than 5 A. The list of the chosen power inductors is shown in Table I. All the inductors have the inductance tolerance of ±20% as specified in the datasheet.

B. Calibration structures

The calibration structures are 30-mm and 55-mm long CBCPW lines that connect two SMA connectors. The model parameters of the SMA connector [7], interconnects and substrate are optimized in Keysight ADS [8] to fit the measured S-parameters of the calibration structures which are obtained after the VNA is calibrated up to the tips of the VNA cable by the SMA calibration set. The CBCPW lines are processed on the FR4 substrate with the relative permittivity and dielectric loss of 5.05 and 0.024, respectively.

Copyright (C) 2019 IEEE. Personal use is permitted.
For any other purposes, permission must be obtained from the IEEE by emailing pubs-permissions@ieee.org

This is the author's version of the article that has been presented at IEEE SPI2019
The editorial version of the paper is available at http://dx.doi.org/10.1109/SaPIW.2019.8781682

TABLE I
LIST OF ANALYZED POWER INDUCTORS WITH DATA FROM DATASHEETS

#	Manufacturer	Model	L, µH	I_{sat}, A	Case size, mm
1	WURTH	74438357010	1.00	9.6	4.1×4.1×3.1
2	BOURNS	SRP4020FA-1R0M	1.00	8.0	4.1×4.1×1.9
3	MURATA	FDSD0420-H-1R0M	1.00	9.0	4.2×4.2×2.0
4	COILCRAFT	XEL4020-102MEB	1.00	9.0	4.0×4.0×2.1
5	BOURNS	SRP4020FA-R47M	0.47	14.0	4.1×4.1×1.9
6	BOURNS	SRP4020FA-R68M	0.68	11.6	4.1×4.1×1.9
7	BOURNS	SRP4020FA-R82M	0.82	9.0	4.1×4.1×1.9
8	BOURNS	SRP4020FA-1R0M	1.00	8.0	4.1×4.1×1.9
9	BOURNS	SRP4020FA-1R2M	1.20	7.5	4.1×4.1×1.9
10	BOURNS	SRP4020FA-1R5M	1.50	7.5	4.1×4.1×1.9
11	BOURNS	SRP4020FA-2R0M	2.00	5.0	4.1×4.1×1.9
12	BOURNS	SRP4020FA-2R2M	2.20	4.8	4.1×4.1×1.9
13	BOURNS	SRP4020FA-3R3M	3.30	5.3	4.1×4.1×1.9
14	BOURNS	SRP4020FA-4R7M	4.70	4.0	4.1×4.1×1.9
15	BOURNS	SRP4020-1R0M	1.00	6.0	4.8×4.0×2.0
16	BOURNS	SRP5015TA-1R0M	1.00	9.0	5.7×5.2×1.3
17	BOURNS	SRP5030T-1R0M	1.00	11.0	5.7×5.2×2.8
18	BOURNS	SRP7030-1R0M	1.00	13.5	7.6×6.5×3.2

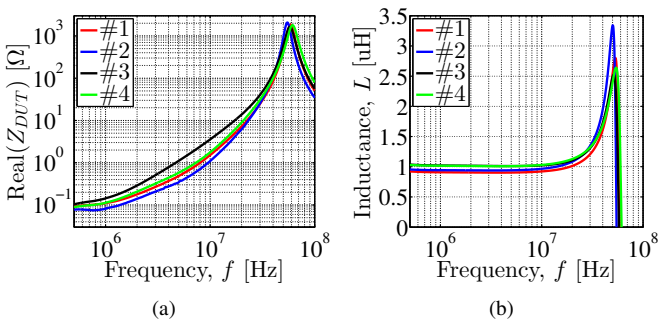

Fig. 1. Inductor set 1: (a) real part and (b) apparent inductance.

C. S-parameter measurement setup

Two-port "shunt" measurement setup is designed to obtain the impedance characteristics of the DUTs [5]. Firstly, the S_{ij} parameters of each power inductor are measured using the designed measurement setup. Secondly, the parasitics of the test fixture are de-embedded from the measured S_{ij} parameters to obtain the S_{ij} parameters of the DUT. Thirdly, the z_{ij} parameters are calculated from the measured S_{ij} parameters of the DUT [9]. The two-port "shunt" measurement method can be represented by the T-model network [5], and the impedance of the extracted inductor model, Z_{DUT}, is calculated as $Z_{DUT} = (z_{12} + z_{21}) / 2$. Finally, the real part, apparent inductance L and Q factor against frequency are calculated from the impedance as: $L = \text{imag}(Z_{DUT})/(2\pi f)$ and $Q = \text{imag}(Z_{DUT}) / \text{real}(Z_{DUT})$.

III. MEASUREMENT RESULTS

A. Frequency-domain characterization

The real part and apparent inductance for the three power inductor sets are shown in Figs. 1, 2 and 3. The real part of the inductor impedance corresponds to the power losses and consists of the winding losses and core losses (resistance). It depends on the manufacturer (i.e core material, set 1) and on the case size (saturation current rating, set 3). The increase of the real part with the inductance as observed for the inductor set 2 is due to the more windings that are used to achieve larger inductance. The plots of the apparent inductance against the frequency show approximately constant inductance for frequencies lower than the self resonant frequency (SRF). As frequency approaches SRF, the apparent inductance increases because the reactance is larger than predicted by $X = j\omega L$.

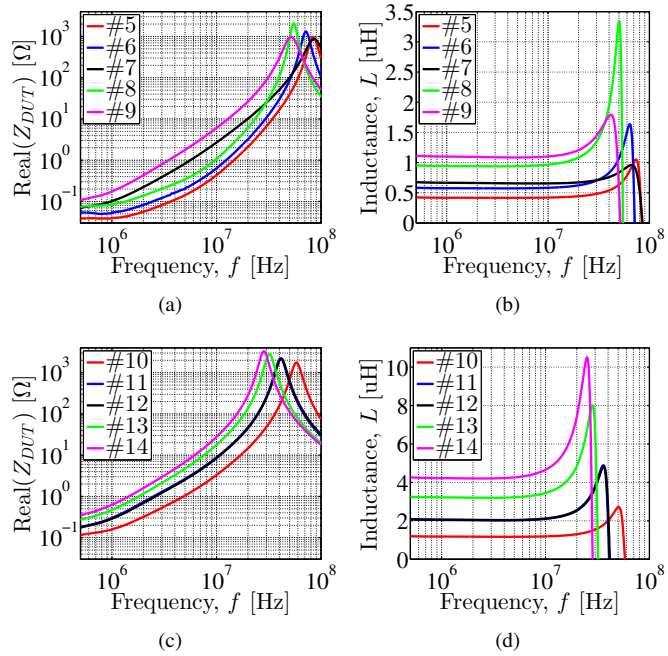

Fig. 2. Inductor set 2: (a), (c) real part and (b), (d) apparent inductance.

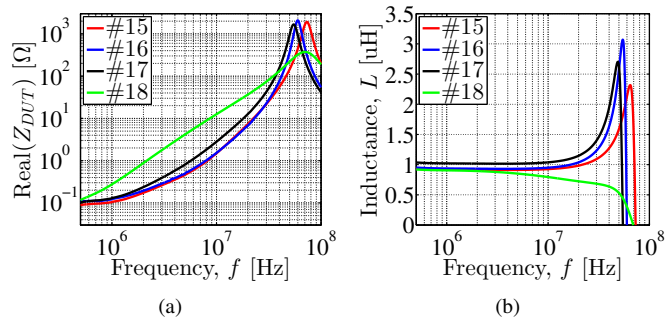

Fig. 3. Inductor set 3: (a) real part and (b) apparent inductance.

The Q factor against the frequency for the three inductor sets is shown in Fig. 4. The Q factor significantly varies between the inductors from different manufacturers (set 1, Fig. 4(a)). Furthermore, inductors with larger saturation current ratings have larger case size, i.e. larger power losses and the Q factor gets lower for the same inductance value (set 3, Fig. 4(d)). All three inductor sets show that the frequency of the maximum Q factor largely depends on the inductor parameters, such as inductance, manufacturer and case size.

Copyright (C) 2019 IEEE. Personal use is permitted.
For any other purposes, permission must be obtained from the IEEE by emailing pubs-permissions@ieee.org

This is the author's version of the article that has been presented at IEEE SPI2019
The editorial version of the paper is available at http://dx.doi.org/10.1109/SaPIW.2019.8781682

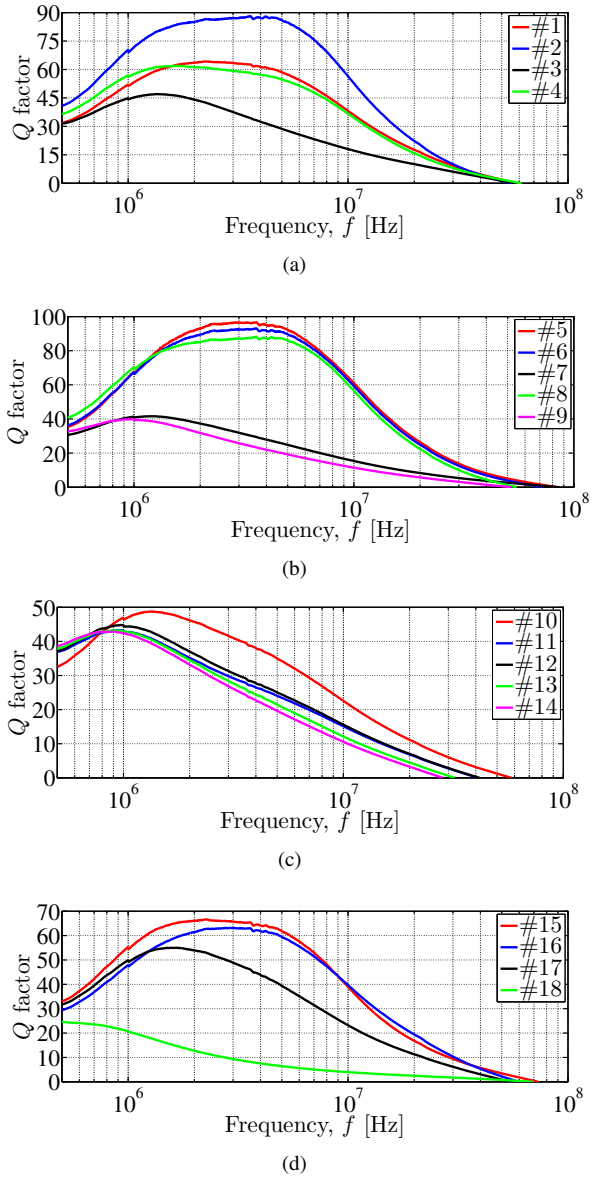

Fig. 4. Q factor vs. frequency for: (a) set 1, (b), (c) set 2 and (d) set 3.

TABLE II
MEASUREMENTS VS. MODEL: INDUCTANCE, Q FACTOR AND SRF

#	Measurements			Model		
	L, µH	Q	SRF, MHz	L, µH	Q	SRF, MHz
1	0.91	52	58.9	1.00	-/-	-/-
2	0.94	70	54.9	1.00	116	62.2
3	1.02	45	57.7	1.00	49	64.0
4	1.02	57	61.3	1.00	-/-	-/-
5	0.42	68	84.1	0.47	117	104.5
6	0.58	67	71.6	0.68	119	82.5
7	0.67	41	86.1	0.82	127	72.3
8	0.94	70	54.9	1.00	116	62.2
9	1.10	40	51.9	1.20	112	56.8
10	1.18	47	58.2	1.50	114	48.9
11	2.06	43	41.0	2.00	113	40.9
12	2.14	45	41.4	2.20	114	38.7
13	3.22	43	32.2	3.30	91	30.0
14	4.22	42	28.3	4.70	79	24.8
15	0.92	55	73.3	1.00	-/-	84.9
16	0.94	48	59.9	1.00	154	67.8
17	1.02	50	54.6	1.00	225	67.5
18	0.91	21	70.4	1.00	31	76.6

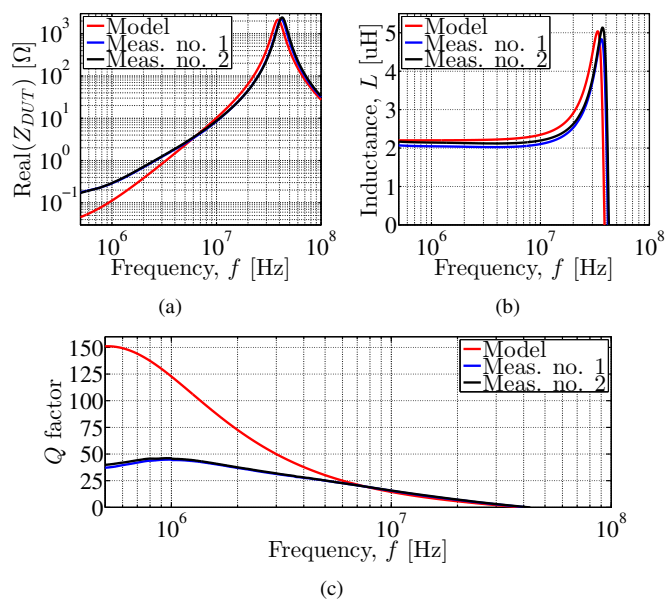

Fig. 5. Inductor #12: (a) real part, (b) apparent inductance and (c) Q factor.

B. Measurements vs. model

The inductance L and Q factor (at 1 MHz which is the switching frequency of the class-E resonant converter used for validation as described in Section IV) as well as SRF extracted from measurements and from the models available at the manufacturer's websites are listed in Table II. The significant difference between the measurements and the model proves that the accurate characterization of the inductors is important for the proper design methodology of the resonant converters.

The comparison of the real part, apparent inductance and Q factor between the two measured samples and the model of the inductor #12 (SRP4020FA-2R2M from Bourns, used for validation as described in Section IV) is shown in Fig. 5. The significant discrepancy for the Q factors can be attributed to the larger real part for the measured than the modelled data.

IV. OPERATION OF THE CLASS-E RESONANT CONVERTER

The impact of the Q factor on the characteristics of the converter is analyzed by the simulations. Two class-E resonant converters are designed. The topology of the converters is shown in Fig. 6. The converters operate at 12-V input voltage, 5-V output voltage, 1-A output current and 1 MHz switching frequency. The design of the converters is performed by the state-of-the-art methodology presented in [1]. The MOSFET is modelled by a switch with $R_{ds,on}$ equal to 0.18 Ω, diode is modelled by a switch with the on-state voltage of 0.5 V and $r_{d,on}$ equal to 0.05 Ω, the capacitors are ideal, while the inductors are modelled by the series RL circuit.

Copyright (C) 2019 IEEE. Personal use is permitted.
For any other purposes, permission must be obtained from the IEEE by emailing pubs-permissions@ieee.org

This is the author's version of the article that has been presented at IEEE SPI2019
The editorial version of the paper is available at http://dx.doi.org/10.1109/SaPIW.2019.8781682

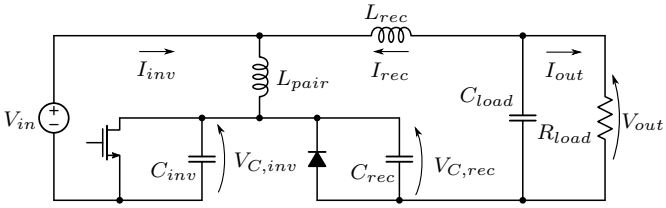

Fig. 6. Analyzed class-E resonant converter [1].

The first converter is designed using the values of the inductor #12, extracted from the measurements. The measured inductance is 2.14 uH and Q factor is 45 at the frequency of 1 MHz. Denormalized values of the circuit obtained by [1] are: C_{inv} = 18.6 nF, C_{rec} = 7.2 nF, L_{rec} = L_{pair} = 2.14 µH. The duty cycle of the control signal is set to 35%. The second converter is designed using the values of the inductance and Q factor extracted from the model of the inductor available at the manufacturer's website [10]. The extracted inductance is 2.2 uH and Q factor is 114 at the frequency of 1 MHz. Denormalized values of the circuit obtained by [1] are: C_{inv} = 17.2 nF, C_{rec} = 5.7 nF, L_{rec} = L_{pair} = 2.2 µH.

The two converters are simulated by SPICE. The inductance and Q factor of the inductors is set to 2.14 µH and 45 (i.e. to the measured values), respectively, in the simulations of both converters. In this way, the impact of these parameters is evaluated. The output voltage of the first converter obtained by the simulations is 5.03 V, while for the second it is 5.13 V. The simulated characteristic waveforms are shown in Fig. 7, for both converters. The ZVS and ZVDS conditions are not satisfied for the converter designed using the inductance and Q factor different than the actual value, which proves the importance of the accurate characterization of the inductors. Additionally, the impact of the Q factor and $\pm 20\%$ variation of L (nominal 2.2 µH) on the output voltage is shown in Fig. 8. The analysis is performed in SPICE and the results show the large impact of the inductor parameters on the output voltage of the analyzed resonant converter.

V. Conclusion

The Q factor of seventeen shielded ferrite-core power inductors is extracted from the S-parameter measurements in the frequency range from 500 kHz to 100 MHz. The variation of the Q factor is observed for the different manufacturers, inductance values and inductor case sizes (saturation currents). The output voltage drop as well as improper operation of the class-E resonant converter is observed when the inductance or Q factor different from the actual values are used in the design methodology. Therefore, the accurate estimation of the power inductor characteristics is important for the exact analytical-based design of the class-E resonant converters.

Acknowledgement

This work is supported in part by the Croatian Science Foundation (HRZZ) within the project Advanced design methodology for switching DC-DC converters.

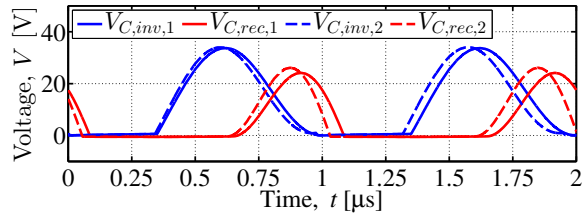

(a)

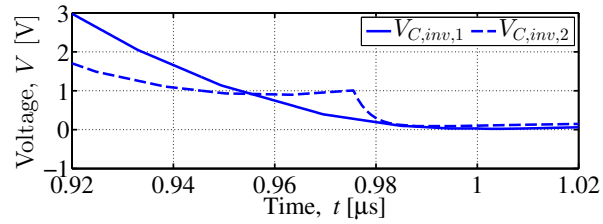

(b)

Fig. 7. (a) Simulated voltage waveforms and (b) enlarged turn-on event.

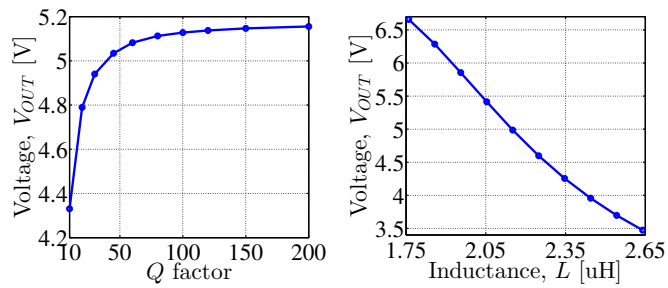

(a) (b)

Fig. 8. Simulated output voltage against: (a) Q factor and (b) inductance. The converter is designed for $Q = 45$ and $L = 2.14$ µH.

References

[1] N. Bertoni, G. Frattini, R. G. Massolini, F. Pareschi, R. Rovatti, and G. Setti, "An Analytical Approach for the Design of Class-E Resonant DC-DC Converters," *IEEE Transactions on Power Electronics*, vol. 31, no. 11, pp. 7701–7713, Nov 2016.

[2] N. Bertoni, G. Frattini, P. Albertini, F. Pareschi, R. Rovatti, and G. Setti, "A First Implementation of a Semi-Analytically Designed Class-E Resonant DC-DC Converter," in *IEEE International Symposium on Circuits and Systems (ISCAS)*, May 2015, pp. 221–224.

[3] J. Wei and Z. Wang, "Frequency-Independent T Equivalent Circuit for On-Chip Spiral Inductors," *IEEE Electron Device Letters*, vol. 31, no. 9, pp. 933–935, Sept 2010.

[4] I. Novak, "Measuring MilliOhms and PicoHenrys in Power-Distribution Networks," in *DesignCon 2000, Santa Clara, CA, USA*, Feb. 2000.

[5] J. Bačmaga, R. Blečić, R. Gillon, and A. Barić, "High-Frequency Modelling of Surface-Mount Power Inductor Used in Switching DC-DC Converters," in *IEEE 20th Workshop on Signal and Power Integrity (SPI)*, May 2016, pp. 1–4.

[6] R. N. Simons, *Coplanar Waveguide Circuits, Components, and Systems*, 1st ed. John Wiley, 2001.

[7] T. Mandic, R. Gillon, B. Nauwelaers, and A. Baric, "Characterizing the TEM Cell Electric and Magnetic Field Coupling to PCB Transmission Lines," *IEEE Trans. on EMC*, vol. 54, no. 5, pp. 976–985, Oct 2012.

[8] Keysight Technologies, *ADS 2015, Simulation-Analog RF*, 2015.

[9] D. M. Pozar, *Microwave engineering*, 3rd ed. Wiley, 2005.

[10] *SRP4020FA Series – Shielded Power Inductors (Equivalent Circuits)*, Bourns, 2018, available at https://www.bourns.com/.

Copyright (C) 2019 IEEE. Personal use is permitted.
For any other purposes, permission must be obtained from the IEEE by emailing pubs-permissions@ieee.org